International Journal of Advanced Technology and Engineering Exploration, Vol 9(93)
ISSN (Print): 2394-5443 ISSN (Online): 2394-7454
http://dx.doi.org/10.19101/IJATEE.2021.875190

Research Article

Experimental and numerical study on the effect of parameters in axial capacity of CFST columns with various L/D ratios

Shaik Madeena Imam Shah[1] and G Mohan Ganesh[2*]
Research Scholar, School of Civil Engineering, Vellore Institute of Technology, Vellore, India[1]
Professor, School of Civil Engineering, Vellore Institute of Technology, Vellore, India[2]

Received: 15-November-2021; Revised: 06-August-2022; Accepted: 12-August-2022

Abstract
Strength as well as behaviour of 16 circular concrete filled steel tube (CFST) sections submitted to axial compressive load was presented in this paper. Specimens having length to diameter (L/D) ratios of 3, 4, 5 and 6 with diameter to thickness (D/t) ratios of 38 as well as 25.33 with same outer diameter of 76 mm and two different wall thickness of 2 mm and 3 mm were considered to study the influence of column parameters and effect of confinement ( ). The ultimate capacities of CFST columns were compared with Eurocode-4, Australian Standards (AS 5100), American Code (AISC 360 - 10) and Chinese code (DBJ13-51) predictions. Results showed that axial compressive loads of specimens with more wall thickness were found to be greater than lesser wall thickness specimens. The parameters that affect the column behaviour directly are relative slenderness ratio (λ) and L/D. Eurocode-4 results found to be conservative, Australian code and American Code underestimated while Chinese code overestimated the section capacity. Further, a finite element model of CFST specimens was developed with ABAQUS to check the accuracy of test results, buckling patterns and displacement curves.

Keywords
Concrete filled steel tube, Confinement, Axial compressive load, Relative slenderness ratio.

1.Introduction
Concrete filled steel tube (CFST) members are highly employed in load carrying structures like bridges, high rise buildings, tunnels and many other structures. With the appearance of fast advances in development of building materials, accompanying high strength concrete and steel in CFST sections acquired incredible recognition [1]. CFST is one of the composite sections that possesses the benefit of carrying a higher load bearing capacity of section with concrete that is enclosed with steel. CFST usually come up with two fundamental benefits against their traditional cement and steel partners. Decreasing the development cost and time as the steel tube gives a stay setup and simple installation of formwork for casting the concrete and the other is the enhancement of mechanical strength and durability of the composite section as the steel tube provide greater confinement to the infilled concrete, [2].

Reinforced concrete sections losses its stiffness by causing cracks when subjected to flexural loadings while concrete enclosed with steel section provides shear capacity. CFST have fabulous strength properties like torsion, compression and bending. Effective confinement is imparted to the core of concrete by steel and prevents the lateral expansion. The capacity of CFST section gets enhanced with the concrete that is inside the steel encasement. This can enhance the bending stiffness of the section. These sections allow no local buckling but gives greater ductility and capacity to the section as they possess greater geometric efficiency [3]. Because of its greater energy absorption, ductility as well as strength, CFST performs well in seismic zones, prompting structural engineers to use them in seismic territories. However, CFST sections exposed to fire shows relatively low axial carrying capacity which is a major disadvantage. This made researchers to study further and find an alternate by adding steel fibres, rebars in the sections. Enormous studies are being conducted to explore the behaviour of CFST specimens by subjecting them to various loads like axial compression, axial bending, impact and blast

*Author for correspondence

loading. Also, the combination of loads like compression and torsion, shear and bending, fire and compression [4−6]. Research on circular CFST subjecting to compression has been executed in recent years that grabbed the attention of many researchers [1, 7, 8].

In the view of practical execution, study on long and stub CFST was also explored [5, 9]. However, these range of parametric studies are not enough to apprehend the mechanism of CFST column. Although, the design specifications from the code books allow the engineers and researchers to forecast the axial capacities of the column, many studies show that design capacities differ from the experimental test results [1, 10]. So, to develop and push the limits of parameters and design specifications, more experimental studies on CFST columns are needed that can enhance the study and behaviour of columns explicitly. "Commentary on the American code specifications for structural steel buildings" [11] highlighted the need of experimental data to finetune the design specifications of CFST columns. Therefore, conducting experiments with varying parameters may enhance the design specifications and expand the limits of parameters in the design codes.

Hence, the objective of this paper was to study the effect of parameters by conducting experiments and numerical analysis, further comparing the results with the standard design codes for checking the accuracy. The frame work of this paper is as per the following: Section 1 is introduction of the paper that contains the background, motive of work, objective and execution of work. Section 2 gives the details of previous research that are related to the current study. Section 3 involves the methodology of the work including the details of design codes, materials and experimental work. Section 4 shows the results of the experimental work along with the ABABQUS modelling and the comparison of results. Section 5 gives the complete discussion on the experimental, parametric and numerical study of the work and thereby conclusions were drawn and complied in section 6.

2.Literature

Many researchers have focused on strength and behaviour of CFST subjected to axial load and bending moment conditions, many design formulae using simplified mechanics model are proposed. Theoretical formulations give less anticipation in the strength of steel tube columns filled with concrete. Codes that are used for foreseeing the section capacity of a CFST column are Chinese code (DBJ13-51), Australian code (AS5100), Eurocode – 4 (EC-4) and American code (AISC 360-10). Studies focused on the predictions of AISC 360-10 based on experimental test results of the column with length/diameter 3-7 and concluded that axial capacity results are conventional for length to diameter (L/D) ratio of 3 [5].

A report shows that the study on stub columns (L/D=3) were found to be very near to EC-4 predictions [12].

Experimental studies conducted on 18 short, medium and long columns exploring the column parameters and confinement effect by comparing them with EC-4 and AISC 360-10 codes [1]. Studies on the effects of confinement on 24 circular, square and strengthened square sections for B/t ratios ranging from 17-150 under uniaxial compression. It is concluded that more confinement effect is observed in circular sections with D/t less than 40 while the same was less in section with B/t greater than 30 [13]. Experimental studies on CFST with various L/D ratios of 2.68 to 4 incorporating ground granulated blast furnace slag in various proportions from 0% to 30% were conducted and concluded that axial capacities of CFST increased with increasing the compressive strength. However, a gap was observed in determining the effect of thickness in axial capacity [14]. Also, 36 CFST columns with thickness of 2.5, 3.5 and 4.5 mm were tested for axial capacity with varying percentage of steel fiber. This study concludes that, adding and increasing steel fibers and thickness, increases the axial capacity [15]. Studies were also conducted on various shapes of CFST that include elliptical, square and rectangle designed using Eurocode-4 (EC4) with different mix proportions of concrete. The conclusions shown in this study are, higher axial load capacity of CFST columns is achieved with higher strength of Self-Compacting Concrete (SCC). Also, limit of slenderness for square and rectangle sections given by EC4 were modified from $52\sqrt{235/f_y}$ to $68\sqrt{235/f_y}$ after conducting a detailed statistical study [16, 17]. Considering the fact that confinement intensifies the axial capacity of CFST columns, an analytical model was proposed by validating 597 experimental test data, showing accuracy in

predicting the load – strain relationships [18]. Based on the study of materials, use of rubber fine aggregate replaced in various volume percentage, 12 CFST columns were tested for compression. Although, the axial test results showed lesser values compared to normal CFST, higher ductility was achieved with more local buckling and hardening post – peak response [19]. Comparison of numerical analysis with experiments of CFST, reinforced cement concrete and slender self – stressing CFST columns with different concrete grade and steel percentage were done showing the satisfactory result in load – displacement plots and ultimate capacities [20, 21]. Experimental investigation on early age loading of CFST done with wrapping of fibre reinforced polymer cloths are compared with normal CFST. Results showed that early age loading can be useful for long term axial carrying capacity specimens [22]. Similar study is seen with geopolymer CFST subjected to compression and bending that are compared for both experiment and numerical analysis. Results showed that, increase in grade of outer steel, thickness and diameter, enhances the resistance to compression and bending [23].

Experimental studies were also conducted on CFST infill with recycled aggregate and steel fibres. Although the recycled aggregate decreases the concrete compressive strength, addition of steel fibres with optimum mix of 1.0% – 1.8% increased the ductility of the columns. Also, the ultimate capacity of the columns was increased by adding steel fibres, increasing the thickness of the steel tube and decreasing the L/D ratios [24−28]. The study continued with proposing a new equation in predicting the ultimate capacity of the specimens and compared with experimental test results which showed accuracy and feasibility in attaining the results [29−31]. The studies were conducted on the bond behaviour of CFST with steel fibres considering the parameters like concrete type, steel tube thickness, strength of concrete and volume percentage of steel fibres. Results showed using steel fibres gives higher bond strength. Also, greater the concrete strength and thickness of steel tube, greater is the bond strength. Proposed equation for determining the bond strength of columns gave accurate results than the existing code results [32−35]. Use of codes in predicting the axial capacity of CFST columns, experimental test data of 230 and 367 circular CFST columns were collected from the literature and their results were compared with code test results. EC4 showed conservative results in predicting the column capacity of the columns [36, 37]. In comparison of experimental test results with design code results and proposed formulae, high accuracy is seen for the results predicted from proposed formulae. Formulae were predicted not only for ultimate axial capacity but also for ultimate strains, stiffness [38, 39], stress – strain relationship [40] and ductility [41] of the CFST specimens.

Based on the literature study and analysis, a notable quantity of experiments with various parameters and geometric properties that act in accordance with the limits applicable for design specifications are published. Therefore, as stated by commentary on the AISC 360 – 10 specification of structural steel buildings [11], new experiments have to enhance the limit of codal design specification.

So, considering the parameters like D/t, L/D, confinement, relative slenderness ratio and Strength Index (SI), the experimental work carried out in this paper has 16 CFST specimens of different L/D and D/t ratios subjected to uniaxial compression that studies the behaviour and strength of column. The parameters affecting the strength and behaviour of CFST are outlined and conclusions were drawn for varied range of parameters. Further, to have keen observation, the section capacities of the columns are compared to predicted column capacities using EC-4 [42], AS5100 [43], DBJ13-51 [44] and AISC 360 – 10 [45] codes.

3.Method

EC4, AS5100, DBJ13-51 and AISC360-10 design codes were used to design the CFST columns. Limit state of design was adapted in all the codes to deliver safety and serviceability by appointing partial safety factors to material properties and loads. All the partial safety factors were considered to be unity for direct comparison with design codes. To have a better understanding, the total working mechanism is shown in the block diagram (*Figure 1*).

3.1Codes and specifications

3.1.1 Eurocode-4

The confinement effect was considered for CFST sections with circular shapes having λ less than 0.5. Equations 1 to 7 show the axial capacity calculation.

$$\lambda = \sqrt{\frac{N_{pl,Rk}}{N_{cr}}} \quad (1)$$

$$N_{pl,Rk} = A_s f_y + A_c f_c \quad (2)$$

$$N_{cr} = \frac{\pi^2 (EI)_{eff}}{(L)^2} \quad (3)$$

$$(EI)_{eff} = E_s I_s + 0.6 E_c I_c \quad (4)$$

The design section capacity of concrete filled circular hollow section is given by:

$$N_u = A_s \eta_a f_y + A_c f_c \left(1 + \eta_c \frac{t}{d} \frac{f_y}{f_c}\right) \quad (5)$$

η_a and η_c are coefficients where eccentricity of loading is zero. They are evaluated as follows:

$$\eta_a = 0.25\,(3 + 2\lambda) \leq 1.0 \quad (6)$$

$$\eta_c = 4.9 - 18.5\,\lambda + 17\,\lambda^2 \geq 0 \quad (7)$$

λ is relative slenderness ratio given in Equation 1.

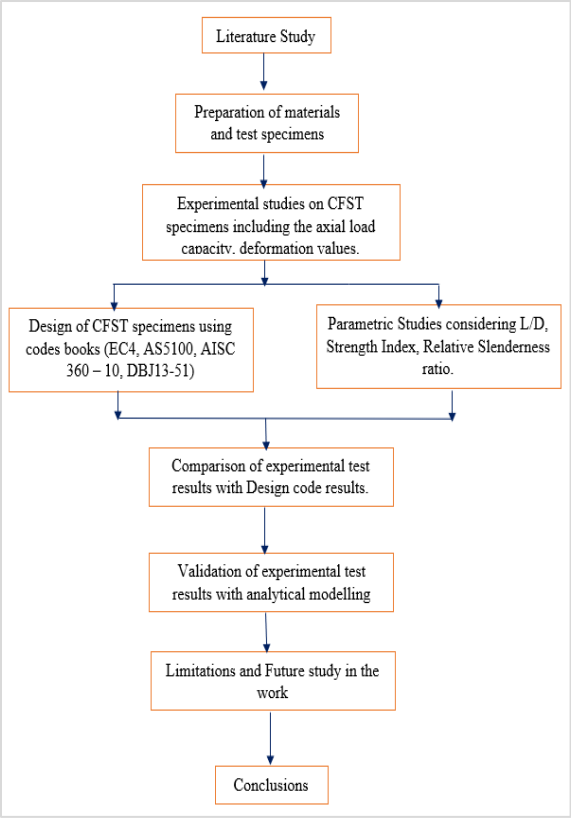

Figure 1 Block Diagram of working mechanism

3.1.2 AS5100

It is an Australian code which adopts rigid plastic theory by assuming stress distribution. Neutral axis of the composite section was found after integration to derive the plastic moment capacity in circular hollow section (CHS). Axial capacity calculations are shown in Equation 8 to 14.

$$\lambda = \sqrt{\frac{N_s}{N_{cr}}} \quad (8)$$

$$N_s = A_s f_y + A_c f_c \quad (9)$$

$$N_{cr} = \frac{\pi^2 (EI)_e}{(L)^2} \quad (10)$$

$$(EI)_e = \phi\, E_s I_s + \phi_c E_c I_c \quad (11)$$

The design section capacity for concrete filled CHS section is given by:

$$N_u = \phi\, A_s \eta_2 f_y + \phi_c A_c f_c \left(1 + \eta_1 \frac{t}{d} \frac{f_y}{f_c}\right) \quad (12)$$

The capacity factors ϕ and ϕ_c are taken as 0.9 and 0.6 respectively.

η_1 and η_2 are the coefficients having eccentric loading zero. They are evaluated as follows:

$$\eta_1 = 4.9 - 18.5\,\lambda_r + 17\,\lambda^2 \geq 0 \quad (13)$$

$$\eta_2 = 0.25\,(3 + 2\lambda) \leq 1.0 \quad (14)$$

3.1.3DBJ13-51

In Chinese code, the section is treated as single solid with material property f_c and correction factor. As per the DBJ13-51, the design section capacity of concrete filled CHS column is given below (Equation 15 to 18).

$$N_u = f_{sc} A_{sc} \quad (15)$$

In which

$$A_{sc} = A_s + A_c \quad (16)$$

$$f_{sc} = (1.14 + 1.02\ \square).\, f_c \quad (17)$$

$$\square = \frac{A_s f_y}{A_c f_c} \quad (18)$$

3.1.4AISC 360-10

The uniaxial compressive load of CFST specimen is calculated based on the slenderness of the member. This code considers the effect of local buckling based on three different classifications and the axial capacities are calculated using Equation 19 to 27.

$$N_u = P_{no}[0.658^{(\frac{P_{no}}{P_e})}] \quad (19)$$

$$\frac{D}{t} < \lambda_p = 0.15 \frac{E_s}{f_y} \quad (20)$$

For compacted section:

$$P_{no} = P_p = A_s f_y + 0.95 A_c f_c \quad (21)$$

For non-compacted section:

$$\lambda_p < \frac{D}{t} < \lambda_r = 0.19 \frac{E_s}{f_y} \quad (22)$$

$$P_{no} = P_p - \frac{P_p - P_y}{(\lambda_r - \lambda_p)^2} (\lambda - \lambda_p)^2 \quad (23)$$

$$P_y = A_s f_y + 0.7 A_c f_c \quad (24)$$

For slender section:

$$\frac{D}{t} > \lambda_r = 0.31 \frac{E_s}{f_y} \quad (25)$$

$$P_{no} = A_s f_{cr} + 0.7 A_c f_c \quad (26)$$

$$f_{cr} = \frac{0.72 f_y}{(\left(\frac{D}{t}\right)\frac{f_y}{E_s})^{0.2}} \quad (27)$$

3.2 Materials used

Outer diameter of 76 mm steel tube was used with 2 mm and 3 mm wall thicknesses. The main intension of selecting two different wall thicknesses was to investigate the exploits of columns with distinct

confinement effect which is a main parameter that is significant for both rectangular and circular cross sections shown in Equation 18. Ordinary Portland cement with 53 grade manufactured by Zuari cement was used in the casting of concrete. As the diameter of the steel tubes is small, the coarse aggregate passing through 12.5 mm sieve and retaining in 10 mm were used. Hence, to have a good flow of concrete, SCC of M30 grade was obtained using European federation of national associations representing for concrete (EFNARC) code through trail mixes. The SCC has achieved all the possible requirements as specified by the code. The fresh properties of SCC are shown in *Table 1*. Three concrete specimens were cured for 28 days and average compressive strength obtained was 38.6 MPa. This range of concrete mix grade was chosen for column testing that was close to specified code design requirements and far from the limit.

3.3 Test specimens

Sixteen CFST columns were selected for this study with outer diameter of 76 mm in which 8 specimens had 2 mm wall thickness with diameter to thickness ratio of 38 and length to diameter ratio of 3, 4, 5 and 6. Similarly, remaining 8 specimens had wall thickness of 3 mm with diameter to thickness ratio of 25.33 and length to diameter ratio of 3, 4, 5 and 6. For each L/D ratio, 2 specimens were casted and tested for finding the uni axial compression and the average load of both specimens were noted. The specimens were named with an identity such as 76D-2t and 76D-3t which indicates 76 mm outer diameter, 2 mm and 3 mm wall thickness respectively. The D/t ratios of steel columns were chosen within the limit specified by codes to avoid the premature buckling failure of the specimens. The limits of parameters prescribed by the codes chosen for this investigation is seen in *Table* 2. Physical properties of the specimens are given in *Table* 3 which consists of length to diameter, thickness (t), outer diameter (D), concrete compressive strength (f_c), yield strength (f_y), area of steel tube (A_s) area of concrete (A_c), confinement factor ( ), relative slenderness ratio (λ) and SI. Before filling the SCC in to the column specimen, the base was machined to ensure the maximum uniformity. All the specimens were painted before curing in order to avoid corrosion.

Figure 2 CFST Columns

The inner surface was brushed and cleaned to have smooth contact between steel and concrete. One end of the steel tube was attached to a base plate before filling self-compacting concrete. The top surface of the specimen was flatted before testing. This was achieved by filling extra layer of concrete on the top surface and kept in curing tank. Before testing, the columns were machined to chip off the extra layer of concrete. Base and top surfaces were made smooth and flat. *Figure* 2 shows CFST specimen used for testing after 28 days of curing. All the CFST specimens were carefully centred to avoid eccentric loading in a 1000 kN universal testing machine. Base plates at the top and bottom of the specimens were placed to ensure the uniform loading for concrete and steel which is in *Figure* 3. The dial gauge was fixed beside the specimen to note the axial deformation values at different loadings. Axial load versus deformation values of each specimen were recorded to study the column behaviour.

4.Results

This section gives the test results of CFST columns. Maximum load carrying capacity, axial load versus deformation curves along with L/D ratio, SI and relative slenderness ratio is discussed.

The parameter used to study the performance of CFST is SI which is defined as follows (Equation 28):

$$SI = \frac{N_u}{A_s f_y + 0.85 A_c f_c} \quad (28)$$

Figure 3 Specimen testing

N_u is determined either by experiment or code predictions. The factor 0.85 is used to compensate uncertainties in concrete which is used to calculate the capacity of CFST section. SI of the columns is given in *Table* 3.

4.1Failure shapes of the columns

Specimens having L/D ratio of 3 failed due to crushing of concrete and outward swelling of steel tube which is dominant in specimens having steel tube thickness of 2 mm as shown in *Figure* 4, whereas columns of L/D 4 and 5 failed due to outward buckling. Global buckling failure was observed in columns having L/D = 6. All the above failures are seen in *Figure* 4.

4.2 Effect of axial capacities in columns

The axial capacities of the columns increased with increase in wall thickness of the steel tube. In comparison of 2 mm and 3 mm wall thickness, 3 mm thick steel tube showed an increment of 19.70%, 15.03%, 14.43% and 18.70% in axial capacities for the specimens with length to diameter ratio of 3, 4, 5 and 6 respectively which is because of more area of steel and its confinement effect. Steel columns having 2 mm wall thickness showed a decrement of 3.35%, 7.59% and 15.3% in axial capacities for L/D of 4, 5 and 6 respectively when compared to L/D of 3. Similarly, 7.74%, 12.61% and 16.4% decrement in axial capacities were observed in 3 mm thick steel tube columns with length to diameter ratio of 4, 5 and 6 respectively when compared to L/D of 3.

Table 1 Fresh properties of SCC as per EFNACR code

Cement (Kg/m^3)	FA (Kg/m^3)	CA (Kg/m^3)	W/C	SP (%)	Slump flow (mm)	V- Funnel	f_c (MPa)
450	740	810	0.46	0.85	605	6 Sec	38.6

Table 2 The range of parameters those are applicable for different code

Parameter	EC4	AS5100	DBJ13-51	AISC 360-10
Diameter to thickness limit	$90\left(\frac{235}{f_y}\right)$	$90\left(\frac{235}{f_y}\right)$	$150\left(\frac{235}{f_y}\right)$	$\lambda_p = 0.15\frac{E_s}{f_y}$
Yield strength (MPa)	$235 \le f_y \le 460$	$200 \le f_y \le 450$	$235 \le f_y \le 420$	$f_y \le 530$
Compressive strength (MPa)	$20 \le f_c \le 60$	$25 \le f_c \le 65$	$20 \le f_c \le 50$	$21 \le f_c \le 70$
Relative slenderness	$\lambda \le 2.0$	$\lambda \le 2.0$	-	-

Table 3 Summary of properties of specimens in experiments

Column	L/D	t (mm)	D/t	f_c (MPa)	f_y (MPa)	A_s (mm^2)	A_c (mm^2)	□	N_e (kN)	λ	SI
76D-2t	3	2	38	38.6	255	464.95	4071.51	0.75	354.5	0.124	1.405
76D-2t	4	2	38	38.6	255	464.95	4071.51	0.75	342.5	0.165	1.358
76D-2t	5	2	38	38.6	255	464.95	4071.51	0.75	329	0.207	1.304
76D-2t	6	2	38	38.6	255	464.95	4071.51	0.75	307	0.248	1.217
76D-3t	3	3	25.3	38.6	255	688.01	3848.46	1.18	424.5	0.119	1.407
76D-3t	4	3	25.3	38.6	255	688.01	3848.46	1.18	394	0.158	1.305
76D-3t	5	3	25.3	38.6	255	688.01	3848.46	1.18	376.5	0.198	1.247
76D-3t	6	3	25.3	38.6	255	688.01	3848.46	1.18	364.5	0.237	1.208

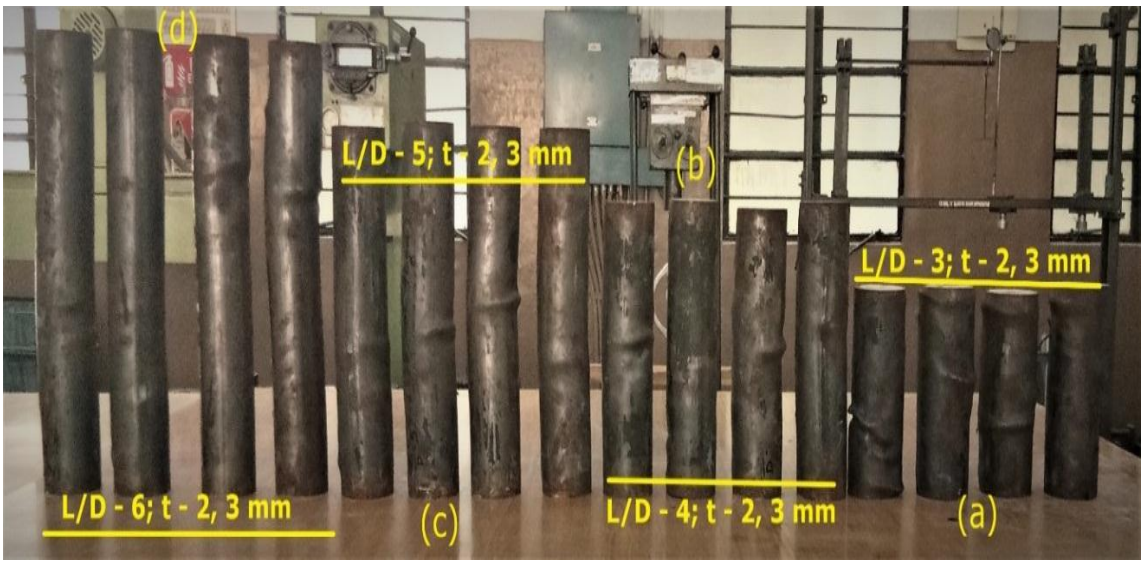

Figure 4 Failure modes of CFST specimens

4.3 Effect of parameters on axial capacities of the columns

All the specimens showed greater axial capacity in 3 mm thick columns having confinement factor 1.18. Hence it can be stated that, as the confinement factor increases, the capacity of the column increases. It is observed from load deformation curves that, there is increase in stiffness for columns of 3mm thick. More deformation and less stiffness are seen in 2 mm thick steel tubes which are shown in *Figure* 5 and *Figure* 6.

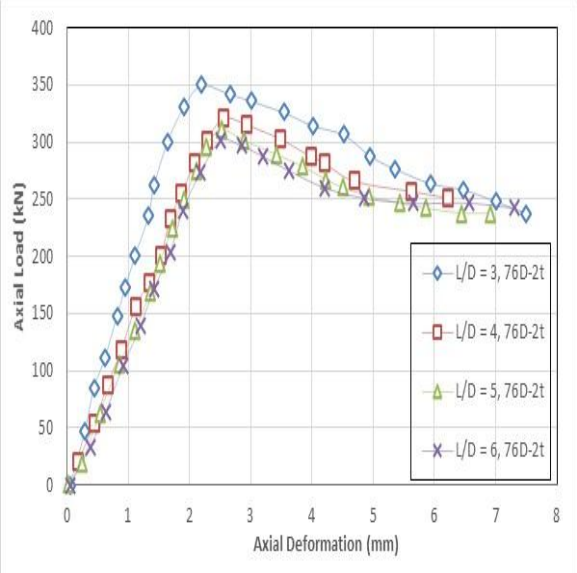

Figure 5 Axial load – deformation curves for 2 mm thick columns

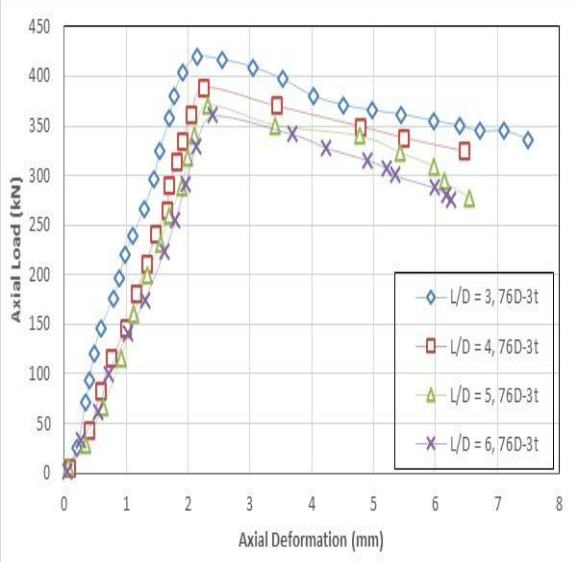

Figure 6 Axial load – Deformation curves for 3 mm thick columns

4.3.1 L/D ratio

Table 4 represents the comparison of test to code results of all the codes. *Figure* 7 shows there is decrease in axial capacity with increase in L/D ratio for specimens having D/t of 38 and 25.33 which were tested after 28 days of curing. It is also observed that as D/t is decreasing, axial capacity of the columns is increasing.

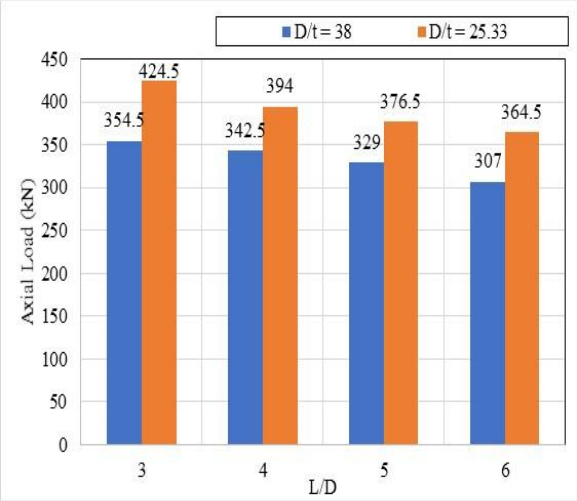

Figure 7 L/D versus Axial load for columns with D/t = 38 and 25.33

4.3.2Strength index

L/D versus SI of the specimens is given in *Figure* 8 in which SI of the columns are decreasing with increasing L/D which clearly shows that this parameter has direct impact on the column capacity.

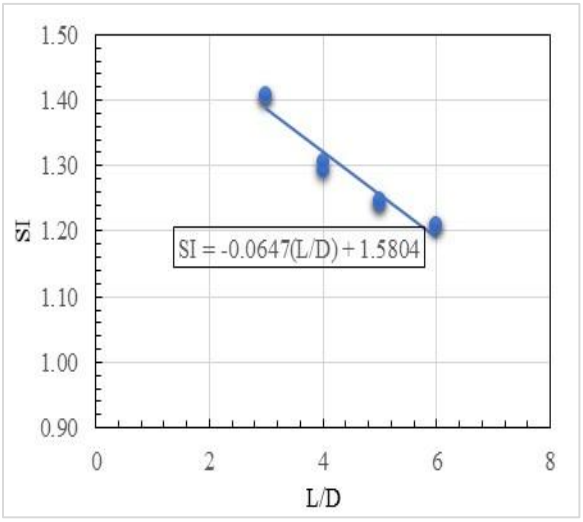

Figure 8 L/D versus SI of the columns

4.3.3Relative slenderness ratio

Figure 9 shows that, the parameter relative slenderness ratio also has straight influence on the axial capacity of the specimen. As relative slenderness is increasing the SI of the column is decreasing.

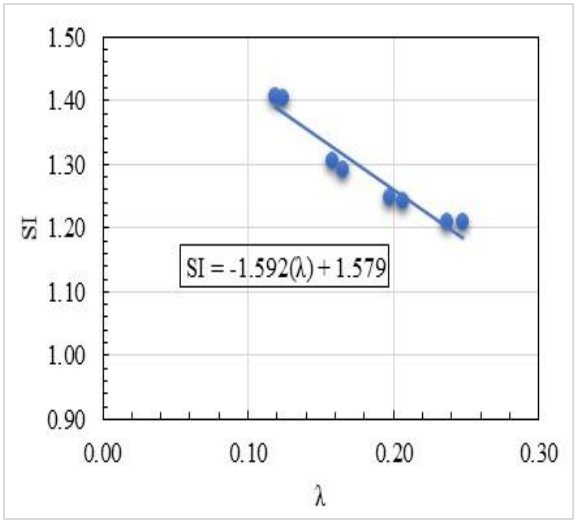

Figure 9 Slenderness ratio versus SI of the column

4.3.4 Code result comparison

Figure 10 and 11 shows L/D versus $N_e/N_{EC4,\ AS5100,\ DBJ13\text{-}51,\ AISC}$ for the columns with Diameter to thickness ratio of 38 and 25.33 as mentioned in the *Table* 4. *Figure* 12 shows relative slenderness ratio versus $N_e/N_{EC4,\ AS5100,\ DBJ13\text{-}51,\ AISC.}$ It is observed from the figures that as L/D is increasing, the predicted values of $N_e/N_{AS5100,\ DBJ,\ AISC}$ are reduced. Whereas EC4 has standard predictions for all columns and showed conservative results which makes a clear conclusion that EC4 gives conservative results in estimating the column carrying capacity. The similar trend was observed for the relative slenderness ratio versus $N_e/N_{EC4,\ AS5100,\ DBJ,\ AISC.}$

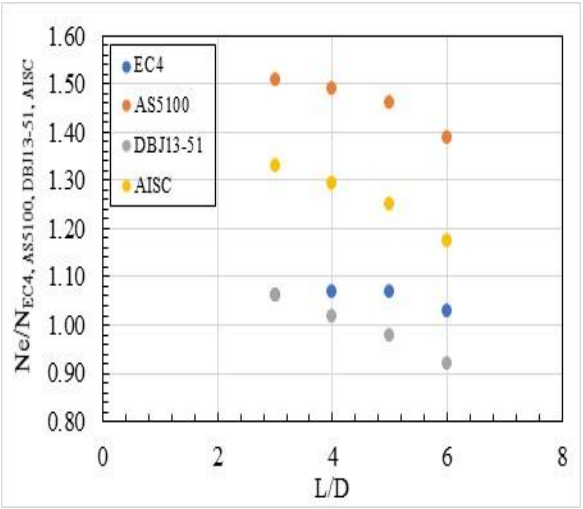

Figure 10 L/D versus N_e/N_c for columns with D/t = 38

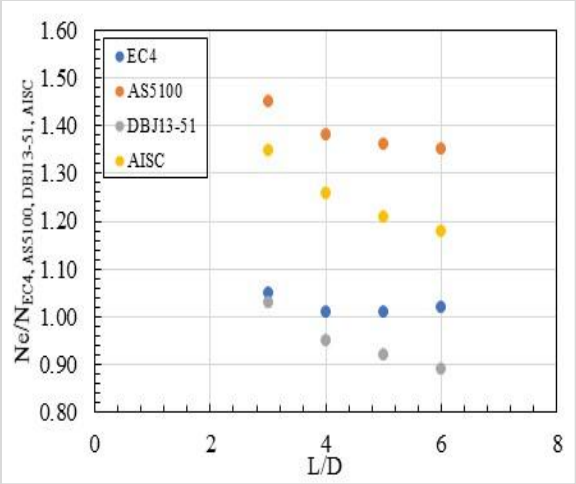

Figure 11 L/D versus N_e/N_c for columns with D/t = 25.33

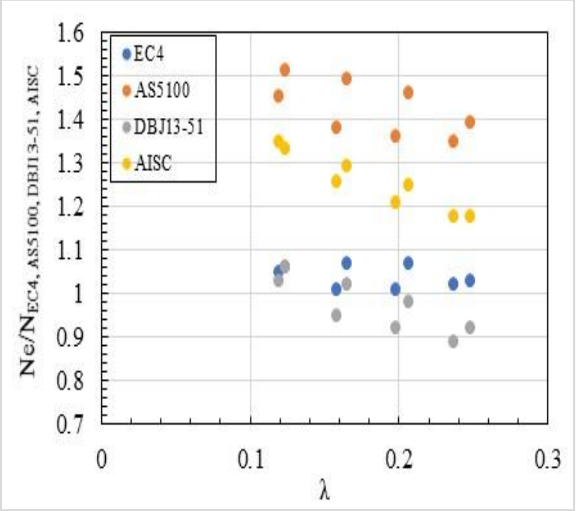

Figure 12 Relative slenderness ratio versus N_e/N_c of the columns

4.4 ABAQUS/CAE modelling

To check the accuracy of the experimental test data of all the 16 CFST columns, finite element analysis (FEA) was done using ABAQUS software by developing the models of CFST specimens. Failure modes, buckling patterns, axial load versus displacement curves were generated and compared with experimental test results.

Results showed maximum difference of 6% compared to experimental results. *Figure* 13 shows load versus deflection curve of 2-mm thick specimen with L/D – 5 and 3-mm thick specimen of L/D – 6 which found to be the best comparison among all the specimens. Buckling pattern and failure mode of

experimental and FEA model for L/D – 5 with 2 mm thickness can be seen in *Figure* 14.

Having the complete study of experimental test results with FEA modelling, it is confirmed that results were very near to accuracy for all the CFST specimens and hence, the established FEA modelling can be used for further parametric studies. Axial load results of experimental and FEA are shown in *Table* 5. Mean value of 0.968, standard deviation (SD) of 0.019 and coefficient of variance (COV) of 0.020 were recorded for all the specimens.

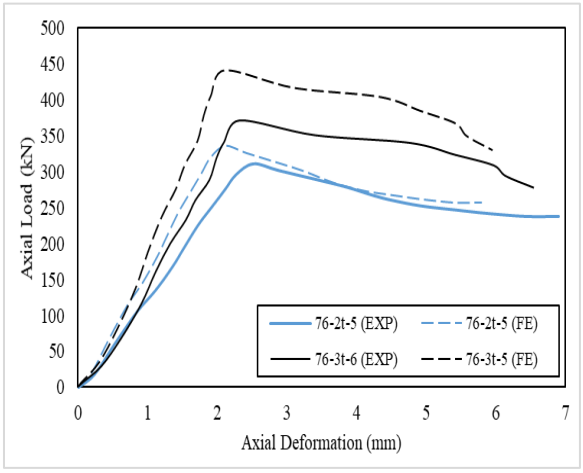

Figure 13 Comparison of axial load versus axial deformation curves for experimental and FEA modelling

Figure 14 Comparison of failure mode of experimental and FE model of CFST

5.Discussion

This section summarizes the findings, interpretations, recommendations along with future direction of the study.

Impact of parameters like relative slenderness ratio (λ), confinement factor (□), L/D, D/t, SI is examined with axial carrying capacity of columns as well as test to code values of EC-4 (N_e/N_{EC4}), AS5100 (N_e/N_{AS5100}), DBJ13-51 (N_e/N_{DBJ}) and AISC360-10 (N_e/N_{AISC}).

As the L/D of the column increases, the axial capacity of the specimens tends to decrease. However, the thickness of the specimen allows the column to carry greater axial load due to its higher area of steel and greater confinement. Hence, 3 mm thick steel tube specimens showed high axial load compared with 2 mm thick specimens.

Also, D/t of the specimen showed greater impact on the axial capacity of the specimen. There was a more load carrying capacity of the specimens having D/t of 25.33 compared to 38. However, the parameter L/D showed dominant effect in allowing the axial capacity of the column. SI of the columns decreased as the L/D, relative slenderness ratio and confinement effect are increased.

Comparing all the experimental test results with design codes of EC4, AS5100, DBJ13-51, ASIC 360-10 the results predicted by EC4 code were near to the test results while other code results were either under estimating or over estimating. This was due to the lack of distinction between the parameters like L/D, relative slenderness ratio in the design procedure of that codes. Hence, a greater number of experimental test data is recommended to enhance the design procedure that can give the predicted results near to experimental test results.

As the study focus on the effect of parameters on axial capacity, further work can be elaborated with the effect of diameter on the axial capacity of CFST column which not only improves the experimental data but also enhances the design procedure in code books which can generate more empirical equations for predicting the axial capacity of the columns.

A complete list of abbreviations is shown in *Appendix I.*

Table 4 Comparison of test results to code results

Specimen	L/D	D/t	N_e (kN)	N_{EC4}	N_e/N_{EC4}	N_{AS5100}	N_e/N_{AS5100}	N_{DBJ}	N_e/N_{DBJ}	N_{AISC}	N_e/N_{AISC}
76D-2t	3	38	354.5	331.79	1.06	235.12	1.51	334.36	1.06	266.2	1.33
76D-2t	4	38	342.5	318.9	1.07	229.72	1.49	334.36	1.02	264.91	1.23
76D-2t	5	38	329	307.6	1.07	224.10	1.46	334.36	0.98	263.26	1.18
76D-2t	6	38	307	297.89	1.03	219.90	1.39	334.36	0.92	261.26	1.16
76D-3t	3	25.3	424.5	404.56	1.05	292.2	1.45	410.56	1.03	314.77	1.34
76D-3t	4	25.3	394	386.85	1.01	284.05	1.38	410.56	0.95	313.38	1.25
76D-3t	5	25.3	376.5	371.28	1.01	276.60	1.36	410.56	0.92	311.61	1.20
76D-3t	6	25.3	364.5	357.74	1.02	269.90	1.35	410.56	0.89	309.45	1.17
				Mean	1.04		1.42		0.97		1.23
				SD	0.02		0.06		0.06		0.06
				COV	0.02		0.04		0.06		0.05

Table 5 Comparison of experimental and FEA test results

Specimen	L/D	D/t	N_e (kN)	N_{FE} (kN)	N_e/N_{FE}
76D-2t	3	38	354.5	378.2	0.937
76D-2t	4	38	342.5	357.1	0.959
76D-2t	5	38	329	335.63	0.980
76D-2t	6	38	307	308.83	0.994
76D-3t	3	25.3	424.5	440.14	0.964
76D-3t	4	25.3	394	417.73	0.943

Specimen	L/D	D/t	N_e (kN)	N_{FE} (kN)	N_e/N_{FE}
76D-3t	5	25.3	376.5	378.37	0.995
76D-3t	6	25.3	364.5	375	0.972
			Mean		0.968
			SD		0.019
			COV		0.020

6.Conclusions

This paper provides important details about the strength and behaviour of CFST columns and the parameters that affect them. Sixteen CFST columns were casted and tested. The values were compared with EC4, AS5100, DBJ13-51 AISC360-10 predictions. Columns having wall thickness of 3 mm with L/D of 3 exhibited greater axial compressive load compared to all other specimens. Therefore, it is concluded that specimens having high confinement effect and lower relative slenderness ratio tolerate larger failure loads. Relative slenderness ratio and L/D are the main parameters that effects the axial compressive carrying capacity of the column and has much significance in the design of the specimen. Axial compressive load carrying capacity of CFST columns having higher wall thickness were found to be greater than that of lesser wall thickness which is due to the more area of steel confining the concrete. However, the axial capacity of CFST specimens is inversely proportioned to the L/D ratios. Axial compressive load predicted using EC4, AS5100, DBJ13-51 and AISC 360 – 10 are compared with experimental results. The axial compressive loads calculated using EC4 were very close to the experimental test values and hence it provides conservative results. While, AS5100 and AISC 360 – 10 under-estimated the test results. DBJ13-51 overestimated the column because the parameter L/D had no significance in the design of the columns in the code. All the CFST specimens were modelled using ABAQUS and good agreement was obtained with 6% difference between experimental and FEA results. Established FE model can be used for further parametric studies.

Acknowledgment

The authors feel highly indebted to Chancellor of Vellore Institute of Technology, Vellore, Tamil Nadu and India for providing the opportunity to pursue our research.

Conflicts of interest

The authors have no conflicts of interest to declare.

Author's contribution statement

Shaik Madeena Imam Shah: Conceptualization, investigation, data curation, writing – original draft, writing -review and editing. **Dr. G Mohan Ganesh:** Study conception, design, data collection, supervision, investigation on challenges and draft manuscript preparation.

References

[1] Ekmekyapar T, Al-eliwi BJ. Experimental behaviour of circular concrete filled steel tube columns and design specifications. Thin-Walled Structures. 2016; 105:220-30.

[2] Evirgen B, Tuncan A, Taskin K. Structural behavior of concrete filled steel tubular sections (CFT/CFSt) under axial compression. Thin-Walled Structures. 2014; 80:46-56.

[3] Han LH, You JT, Lin XK. Experimental behaviour of self-consolidating concrete (SCC) filled hollow structural steel (HSS) columns subjected to cyclic loadings. Advances in Structural Engineering. 2005; 8(5):497-512.

[4] Lai Z, Varma AH, Zhang K. Noncompact and slender rectangular CFT members: experimental database, analysis, and design. Journal of Constructional Steel Research. 2014; 101:455-68.

[5] Lai Z, Varma AH. Noncompact and slender circular CFT members: experimental database, analysis, and design. Journal of Constructional Steel Research. 2015; 106:220-33.

[6] Han LH, Li W, Bjorhovde R. Developments and advanced applications of concrete-filled steel tubular (cfst) structures: members. Journal of Constructional Steel Research. 2014; 100:211-28.

[7] Abed F, Alhamaydeh M, Abdalla S. Experimental and numerical investigations of the compressive behavior of concrete filled steel tubes (CFSTs). Journal of Constructional Steel Research. 2013; 80:429-39.

[8] Yu ZW, Ding FX, Cai CS. Experimental behavior of circular concrete-filled steel tube stub columns. Journal of Constructional Steel Research. 2007; 63(2):165-74.

[9] Dundu M. Compressive strength of circular concrete filled steel tube columns. Thin-Walled Structures. 2012; 56:62-70.

[10] Giakoumelis G, Lam D. Axial capacity of circular concrete-filled tube columns. Journal of Constructional Steel Research. 2004; 60(7):1049-68.

[11] Griffis LF, Hajjar JL, Hazel PM, Janowiak MV, Kloiber RC, Larson LF, et al. Specification-for-structural-steel-buildings-360-10. pdf.

[12] Wang W, Ma H, Li Z, Tang Z. Size effect in circular concrete-filled steel tubes with different diameter-to-

thickness ratios under axial compression. Engineering Structures. 2017; 151:554-67.
[13] Hu HT, Huang CS, Wu MH, Wu YM. Nonlinear analysis of axially loaded concrete-filled tube columns with confinement effect. Journal of Structural Engineering-ASCE. 2003; 129(10):1322-9.
[14] Ahmad S, Kumar A, Kumar K. Axial performance of GGBFS concrete filled steel tubes. Structures 2020; 23:539-50. Elsevier.
[15] Li N, Lu Y, Li S, Gao D. Axial compressive behaviour of steel fibre reinforced self-stressing and self-compacting concrete-filled steel tube columns. Engineering Structures. 2020.
[16] Liao J, Li YL, Ouyang Y, Zeng JJ. Axial compression tests on elliptical high strength steel tubes filled with self-compacting concrete of different mix proportions. Journal of Building Engineering. 2021.
[17] Chen J, Chan TM, Chung KF. Design of square and rectangular CFST cross-sectional capacities in compression. Journal of Constructional Steel Research. 2021.
[18] Zhu JY, Chen J, Chan TM. Analytical model for circular high strength concrete filled steel tubes under compression. Engineering Structures. 2021.
[19] Shen M, Huang W, Liu J, Zhou Z. Axial compressive behavior of rubberized concrete-filled steel tube short columns. Case Studies in Construction Materials. 2022.
[20] Reddy GS, Bolla M, Patton ML, Adak D. Comparative study on structural behaviour of circular and square section-concrete filled steel tube (CFST) and reinforced cement concrete (RCC) stub column. Structures 2021; 29:2067-81. Elsevier.
[21] Liu Z, Lu Y, Li N, Zong S. Experimental investigation and computational simulation of slender self-stressing concrete-filled steel tube columns. Journal of Building Engineering. 2022; 48:103893.
[22] Zhang J, Ma L, Zhou C, Lee D, Filippou FC. Experimental study of axial compression behavior of circular concrete-filled steel tubes after being loaded at an early age. Construction and Building Materials. 2021.
[23] Fang H, Visintin P. Structural performance of geopolymer-concrete-filled steel tube members subjected to compression and bending. Journal of Constructional Steel Research. 2022.
[24] Liu Z, Lu Y, Li S, Yi S. Behavior of steel tube columns filled with steel-fiber-reinforced self-stressing recycled aggregate concrete under axial compression. Thin-Walled Structures. 2020.
[25] Das CS, Dey T, Dandapat R, Mukharjee BB, Kumar J. Performance evaluation of polypropylene fibre reinforced recycled aggregate concrete. Construction and Building Materials. 2018; 189:649-59.
[26] Butler L, West JS, Tighe SL. The effect of recycled concrete aggregate properties on the bond strength between RCA concrete and steel reinforcement. Cement and Concrete Research. 2011; 41(10):1037-49.
[27] Li LJ, Tu GR, Lan C, Liu F. Mechanical characterization of waste-rubber-modified recycled-aggregate concrete. Journal of Cleaner Production. 2016; 124:325-38.
[28] Yang YF, Han LH. Experimental behaviour of recycled aggregate concrete filled steel tubular columns. Journal of Constructional Steel Research. 2006; 62(12):1310-24.
[29] Lu Y, Liu Z, Li S, Li N. Bond behavior of steel fibers reinforced self-stressing and self-compacting concrete filled steel tube columns. Construction and Building Materials. 2018; 158:894-909.
[30] Li S, Liu Z, Lu Y, Zhu T. Shear performance of steel fibers reinforced self-confinement and self-compacting concrete-filled steel tube stub columns. Construction and Building Materials. 2017; 147:758-75.
[31] Chen P, Wang Y, Zhang S. Size effect prediction on axial compression strength of circular CFST columns. Journal of Constructional Steel Research. 2020.
[32] Dong H, Chen X, Cao W, Zhao Y. Bond behavior of high-strength recycled aggregate concrete-filled large square steel tubes with different connectors. Engineering Structures. 2020.
[33] Dong H, Chen X, Cao W, Zhao Y. Bond-slip behavior of large high-strength concrete-filled circular steel tubes with different constructions. Journal of Constructional Steel Research. 2020.
[34] Wang X, Liu Y, Li Y, Lu Y, Li X. Bond behavior and shear transfer of steel section-concrete interface with studs: testing and modeling. Construction and Building Materials. 2020.
[35] Qu X, Liu Q. Bond strength between steel and self-compacting lower expansion concrete in composite columns. Journal of Constructional Steel Research. 2017; 139:176-87.
[36] Shah SM, Ganesh GM. Influence of parameters on the strength and behavior of concrete filled steel tube specimens subjected to axial compression and cyclic loading. Materials Today: Proceedings. 2022; 65(2):629-35.
[37] Wang X, Fan F, Lai J. Strength behavior of circular concrete-filled steel tube stub columns under axial compression: a review. Construction and Building Materials. 2022.
[38] Yu F, Chen L, Bu S, Huang W, Fang Y. Experimental and theoretical investigations of recycled self-compacting concrete filled steel tubular columns subjected to axial compression. Construction and Building Materials. 2020.
[39] Kwan AK, Dong CX, Ho JC. Axial and lateral stress–strain model for concrete-filled steel tubes. Journal of Constructional Steel Research. 2016; 122:421-33.
[40] Lai MH, Song W, Ou XL, Chen MT, Wang Q, Ho JC. A path dependent stress-strain model for concrete-filled-steel-tube column. Engineering Structures. 2020.
[41] Su M, Cai Y, Chen X, Young B. Behaviour of concrete-filled cold-formed high strength steel circular stub columns. Thin-Walled Structures. 2020.

[42] https://www.phd.eng.br/wp-content/uploads/2015/12/en.1994.1.1.2004.pdf. Accessed 10 February 2022.
[43] AS5100. 6. Bridge design—part 6: steel and composite construction. 2004.
[44] Housing and Urban-Rural Development Dept. of Fujian Province. Technical specifications for concrete-filled steel tubular structures (revised version). 2010.
[45] American institute of steel construction. AISC 360-10 Specification for Structural Steel Buildings. 2010.

Shaik Madeena Imam Shah is a Research Scholar and holds M. Tech (2016) in Structural Engineering from Vellore Institute of Technology, Vellore. He is currently pursing PhD from the same. He has 3 years of teaching experience and has published 2 international conference papers and 2 research papers in reputed journals. His area of research interest is Steel Structures, Concrete Technology, Composite Materials and Design of CFST.
Email: shaikmadeena.imam2017@vitstudent.ac.in

G Mohan Ganesh is a Professor (HAG) in Vellore Institute of Technology, Vellore. He holds a PhD in Structural Engineering from IIT Roorkee (2006). He also holds M.E – Structural Engineering from Government college of Technology, Coimbatore (2000). He has 13 years of teaching and research experience in the field of structural engineering and published more than 40 research papers with more than 200 citations and h-index of 7. He collaborated and successfully completed many R & D projects worth of more than 40 Lakhs.
Email: gmohanganesh@vit.ac.in

Appendix I

S. No.	Abbreviation	Description
1	A_s	Area of Steel
2	A_c	Area of Concrete
3	CFST	Concrete Filled Steel Tube
4	CHS	Circular Hollow Section
5	COV	Coefficient of Variance
6	D/t	Diameter/thickness
7	E_c	Elastic Modulus (concrete)
8	E_s	Elastic Modulus (steel)
9	$(EI)_{eff}$	Effective Stiffness
10	EFNARC	European Federation of National Associations Representing for Concrete
11	FEA	Finite Element Analysis
12	f_y	Yield Strength of Steel
13	f_c	Concrete Compressive Strength
14	I_s	Moment of Inertia (steel)
15	I_c	Moment of Inertia (concrete)
16	L	Length of the Specimen
17	L/D	Length/Diameter
18	N_u	Axial Compressive Capacity in Code
19	N_e	Axial Compressive Capacity in Experiments
20	P_{no}	Nominal Compressive Capacity of Composite Section
21	P_e	Euler Critical Load
22	P_p	Plastic Strength of the Section
23	P_y	Yield Strength of Composite Section
24	SCC	Self-Compacting Concrete
25	SD	Standard Deviation
26	SI	Strength Index